Proceedings of the 9th U.S. National and 10th Canadian Conference on Earthquake Engineering
Compte Rendu de la 9ième Conférence Nationale Américaine et
10ième Conférence Canadienne de Génie Parasismique
July 25-29, 2010, Toronto, Ontario, Canada • Paper No 1337

DEVELOPMENT AND VALIDATION OF GROUND-MOTION ATTENUATION RELATIONSHIP FOR LARGE-MAGNITUDE SUBDUCTION EARTHQUAKES

Kusnowidjaja Megawati[*] and Tso-Chien Pan[†]

ABSTRACT

A representative attenuation relationship is one of the key components required in seismic hazard assessment of a region of interest. Attenuation relationships for peak ground acceleration, peak ground velocity and response spectral accelerations for Sumatran megathrust earthquakes, covering M_w up to 9.0, are derived based on synthetic seismograms obtained from a finite-fault kinematic model. The relationships derived are for very hard rock site condition and for a long distance range between 200 and 1500 km. They are then validated with recorded data from giant earthquakes on Sumatran megathrust occurring since year 2000. Close examination of the recorded data shows that spectral shapes predicted by most of the existing attenuation relationships are not particularly suitable for sites where potential seismic hazard is dominated by large-magnitude, distant, earthquakes. Ground motions at a remote site are typically signified by the dominance of long-period components with periods longer than 1 s, whereas the predominant periods from most of the existing attenuation relationships are shorter than 0.6 s. The shifting of response spectrum toward longer period range for distant earthquakes should be carefully taken into account in formulation of future seismic codes for Southeast Asia, where many metropolises are located far from active seismic sources. The attenuation relationship derived in the present study can properly reproduce the spectral shape from distant subduction earthquakes, and could hopefully give insights in formulation of future seismic codes.

Introduction

Singapore and peninsular Malaysia face a unique problem in seismic hazard analysis. The local seismicity itself is very low as evidenced in the fact that all ground tremors felt in the last 50 years originated from distant Sumatran earthquakes (Pan and Sun 1996). Intuitively, it could be postulated that the seismic sources that may potentially affect Singapore and peninsular Malaysia are large-magnitude earthquakes on Sumatran fault and the adjacent subduction zone. The closest distances from Singapore to the fault and megathrust are 400 and 600 km,

[*] Assistant Professor, Earth Observatory of Singapore and School of Civil and Environmental Engineering, Nanyang Technological University, Singapore
[†] Professor, School of Civil and Environmental Engineering, Nanyang Technological University, Singapore

respectively. The highly segmented, right-lateral, Sumatran fault could produce earthquakes with M_w up to 7.8. On the other hand, the megathrust has known to repeatedly produce giant earthquakes with $M_w > 8.0$ (Chlieh *et al.* 2007).

The motivation of the present work originated from the fact that existing attenuation relationships derived for subduction zones in Japan, Taiwan, Cascadia, Alaska, Chile, Mexico, Peru and other parts of the world could not reproduce response spectra from actual data recorded in Singapore from Sumatran subduction earthquakes. This will be elaborated further in a later section. Megawati *el al*. (2005) have derived a set of spectral attenuation relationships for Sumatran subduction earthquakes. The study was based on synthetic seismograms produced using a point-source dislocation model. Although the derived attenuation relationships could estimate actual recorded data for earthquakes with $M_w \leq 7.2$, they were not tested for giant earthquakes because actual recorded data was not available at the time (Megawati *el al*. 2005).

The objective of the present study is to extend the work by Megawati *et al*. (2005) to cover larger magnitude earthquakes. In the present work, synthetic seismograms will be generated using a finite-fault kinematic model, which have been tested for simulating giant subduction earthquakes (Megawati and Pan 2009). The validation of the attenuation relationships derived is made possible by the availability of good quality data recorded in Singapore from giant Sumatran earthquakes in December 2004, March 2005 and September 2007.

Sumatran Megathrust

The Sunda arc, extending over 5,600 km from the Andaman islands in the northwest to the Banda arc in the east, was formed by the convergence between the subducting Indian-Australian plate and the overriding south-eastern Eurasian plate. The Sumatran megathrust of the Sunda arc lies 250 km off western coast of Sumatra island (Figure 1), with both Sumatra and Java islands lying on the Eurasian plate. The convergence is nearly orthogonal to the trench axis south of Java, but it is highly oblique southwest of Sumatra.

Six giant earthquakes ($M_w \geq 8.0$) have occurred along the Sumatran megathrust in the last 250 years, releasing the strain accumulated by the convergence between the two tectonic plates. The rupture zones of these earthquakes are depicted in Figure 1. The earliest of these historical events was that of February 1797 (Natawidjaja *et al*. 2006). The earthquake had an M_w of 8.7 and ruptured the 370-km segment from 1^oS to about 4^oS. This was followed by the giant earthquake of 1833 (M_w 9.0), which ruptured a 500-km-long segment south of Siberut island, and another one in 1861 (M_w 8.5) rupturing a 270-km-long segment beneath Nias island.

Since 1861, no giant earthquake with $M_w \geq 8.0$ had occurred along Sumatran megathrust until 26 December 2004, when the M_w 9.15 Aceh-Andaman earthquake happened (Chlieh *et al*. 2007). This was shortly followed by the M_w 8.6 Nias-Simeulue earthquake on 28 March 2005 (Briggs *et al*. 2006), which has a rupture zone coincident with that of the 1861 event. The latest giant earthquake of M_w 8.4 occurred on 12 September 2007, at 11:10:26 GMT, denoted at Event 10 in Figure 1.

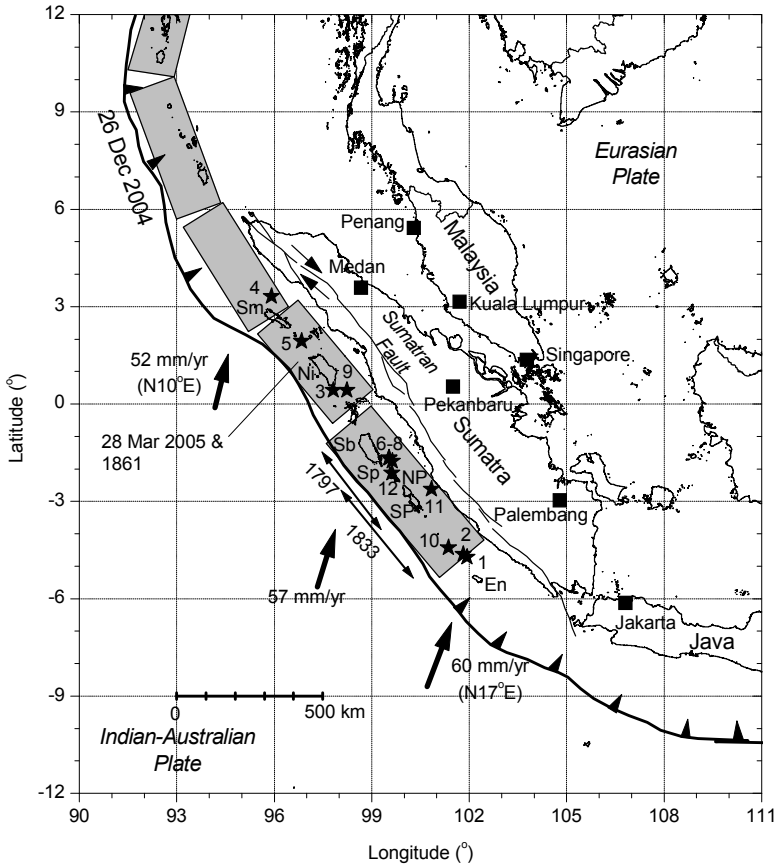

Figure 1. Tectonic setting of Sumatra, together with the epicentres of twelve significant earthquakes occurring on Sumatran megathrust, from January 2000 to December 2007.

Sumatran-Subduction Events Recorded in Singapore

Between January 2000 and December 2007, twelve Sumatran subduction earthquakes had generated substantial ground tremors capable of causing perceptible levels of vibration in Singapore. They include five earthquakes of $M_w \geq 7.9$. The epicentres of these significant earthquakes are plotted in Figure 1. The ground motions from these significant earthquakes are recorded at the broadband Global Seismographic Network (GSN) station in Singapore. Although these twelve sets of ground motions are not sufficient for deriving a representative attenuation relationship empirically, they are useful for validation of the spectral attenuation relationship that will be derived hereafter using synthetic seismograms.

Synthetic Seismograms

A representative response-spectral attenuation relationship, which is a key ingredient in any seismic hazard studies, will be derived based on synthetic seismograms computed for large-magnitude subduction earthquakes along Sumatran megathrust. Six cities in the region, namely Singapore, Kuala Lumpur, Penang, Medan, Pekanbaru and Palembang, are selected as stations where ground motions are to be synthesised. The locations of the cities are shown in Figure 1.

Ground-motion Simulation Method

The ground-motion simulation method used in the present study follows a kinematic method, in which the source rupture is represented using a finite-fault model (Megawati and Pan 2009). The fault plane is subdivided into several subfaults and each subfault is treated as a point source. The rupture starts at the hypocentre and propagates radially outward at a certain rupture velocity, triggering each subfault as the rupture front passes its centre. The ground motions at an observation point produced by the ruptures of individual subfaults are summed with time lags to account for rupture propagation on the fault plane.

The crustal structure representing the whole region of Sumatra and peninsular Malaysia is extracted from the global crustal model CRUST 2.0, which is a $2^o \times 2^o$ global model for the Earth's crust based on seismic refraction data published in the period of 1948 – 1995. The Green's functions are based on synthetics derived from elastic wave-propagation model, which provides proper phasing of body and surface waves.

Source Parameters

Earthquakes with magnitudes ranging from M_w 5 to 9, with an interval of 0.5, are simulated. The strike of Sumatran megathrust is taken to be N320^{o}E, and the dip is 12^o (Chlieh *et al.* 2007). The length and width of the fault plane corresponding to each magnitude level are calculated based on the empirical relationship proposed by Wells and Coppersmith (1994), and they are summarized in Table 1. For each magnitude twelve rupture planes are considered, and they are randomly positioned between latitudes 6^{o}N and 6^{o}S. The upper side of the fault planes is assumed to be exposed on the surface of the uppermost crustal layer. The twelve fault planes for each magnitude level have random rupture patterns, which are constrained by the parameters described below. Each fault plane is subdivided into numerous subfaults, where each subfault is modelled using a point dislocation source. The size of the subfaults for each magnitude is summarised in Table 1.

The source time function of the slip on each subfault is approximated by a ramp function with a source duration of $t_r = L_s/v_r + t_d$, where L_s is the length of the subfault, v_r is the rupture velocity, and t_d is the rise time of the local dislocation. The rise time t_d is equal to D_s/v_d, in which D_s is the slip amplitude and v_d is the slip velocity. The source duration t_r is to reflect the effects of rupture propagation within the subfault and the dislocation rise time.

Table 1. Rupture parameters of simulated Sumatran subduction earthquakes

		M_w 5.0	M_w 6.0	M_w 7.0	M_w 8.0	M_w 9.0
Fault plane						
	Strike	N320^{o}E	N320^{o}E	N320^{o}E	N320^{o}E	N320^{o}E
	Dip	12^o	12^o	12^o	12^o	12^o
	Fault dimensions along the strike and downdip (km × km)	3 × 3	12 × 6	42 × 18	150 × 45	600 × 180
	Subfault size (km × km)	3 × 3	6 × 6	6 × 6	15 × 15	20 × 20
Slip distribution						

	Amplitude	Normally distributed with a coefficient of variance (COV) of 0.2				
	Rake angle	Random value between 60^o and 120^o				
	Slip velocity v_d	Random value between 0.2 and 0.4 m/s				
	No. of asperities	0	0	2	2	2
	Area ratio of asperities	-	-	0.24	0.23	0.22
	Slip contrast of asperities	-	-	2.0	2.0	2.0
	Average slip of the entire rupture plane (m)	0.11	0.44	1.31	4.64	7.61
	Average slip of the asperities (m)	-	-	2.62	9.28	15.22
	Average slip outside the asperities (m)	-	-	0.90	3.25	5.46
Rupture propagation						
	Rupture velocity	Random value between 2.4 and 3.0 km/s				
	Hypocentre	Randomly located along the fault plane, but not within the asperities				

Simulation Results

Figure 2 presents the velocity time histories simulated at Singapore for earthquakes with three different M_w values of 5, 7 and 9. The horizontal ground velocities are aligned in the North-South and East-West directions. The epicentres of the earthquakes are located at about latitude 2^{o}S, and the epicentral distances to Singapore are approximately 650 km. Note that the ground motion shown for each magnitude level represents only one of the twelve random models simulated for that particular magnitude level. The upper cut-off frequency of the simulations is 2 Hz.

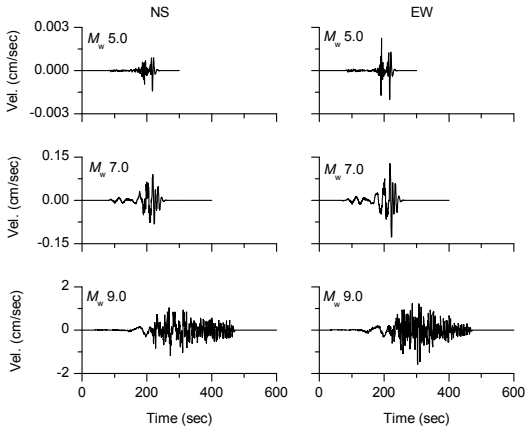

Figure 2. Velocity time histories from three Sumatran subduction earthquakes with M_w values of 5, 7 and 9, simulated for Singapore.

Figure 3 summarises the horizontal PGA simulated for earthquakes with M_w of 6, 7, 8 and 9. The horizontal component is represented by the geometric mean value of the NS and EW components. For each magnitude level, there are 72 data points, resulting from the twelve random rupture models simulated at the six representative cities.

Note that the ground motions are simulated for a shear-wave velocity of 3.4 km/s at the ground surface. This means that the results are for very hard rock sites. For typical rock and soil sites, such as NEHRP site classes A – E, corresponding site response factors, such as those proposed by Boore and Joyner (1997) should be applied.

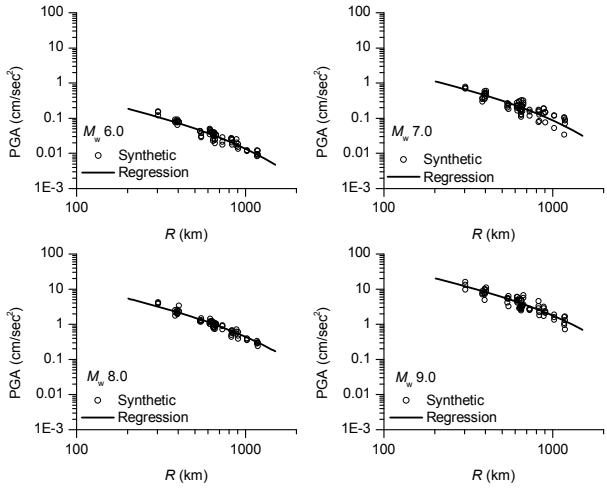

Figure 3. Attenuation relationship of peak ground acceleration for different M_w values of 6, 7, 8 and 9.

Derivation of Attenuation Relationship

The functional form adopted for estimate of the horizontal ground-motion parameters follows the basic principles of wave propagation in elastic media as described below:

$$\ln(Y) = a_0 + a_1(M_w - 6) + a_2(M_w - 6)^2 + a_3 \ln(R) + (a_4 + a_5 M_w)R + \varepsilon_{\ln(Y)} \quad (1)$$

where Y is the geometric mean of the horizontal PGA, PGV or RSA values (5% damping ratio) at various natural periods. The unit for the acceleration values is cm/s^2 and that for velocity is cm/s. M_w is the moment magnitude and R is the distance from the station to the centre of the corresponding fault plane, in km. The quadratic term of $a_2(M_w\text{-}6)^2$ is adopted to account for the fact that the corner period of earthquake source spectrum increases with earthquake magnitude and source area, and the rate of increase of ground motion amplitude Y becomes slower for larger value of M_w (Fukushima 1996). Therefore, the regression coefficient a_2 is expected to have negative values.

Coefficient a_3 in Equation (1) represents the geometrical attenuation rate, whereas a_4 and a_5 account for the anelastic attenuation. The term $\varepsilon_{\ln(Y)}$ is to account for the variations in the PGA, PGV and RSA due to the randomness in source parameters considered in the simulations. The term $\varepsilon_{\ln(Y)}$ has a mean value of 0.0 and a standard deviation value $\sigma_{\ln(Y)}$, representing the standard deviation of the model due to the randomness in the source process.

The regression coefficients of a_0 to a_5 are determined to best fit the simulated data using a least-squares procedure. The procedure minimizes the sum of squared residuals, where the residual is defined as the difference between the ln(Y) simulated and that predicted using Equation (1).

The regression coefficients for PGV, PGA and RSA values at various natural periods of engineering interest are summarized in Table 2, together with the standard deviation values. It should be noted that the values of $\sigma_{\ln(Y)}$, mostly ranging between 0.2 and 0.5, are relatively smaller than the standard deviation values of other attenuation models for subduction earthquakes. For example, Youngs *et al*. (1997) propose standard deviation values of 0.6 – 1.0, Gregor *et al*. (2002) give values of 0.7 – 0.9, Atkinson and Boore (2003) and Lin and Lee (2008) suggest 0.5 – 0.8. It should be understood that the $\sigma_{\ln(Y)}$ in the present study only accounts for the randomness in the source parameters only, and does not include the randomness in the propagation path. For future uses in regional seismic hazard analyses, the $\sigma_{\ln(Y)}$ values in Table 2 need to be increased by about 0.2 to account for the path effects.

Table 2. Regression coefficients of attenuation relationships for PGV (cm/s), PGA (cm/sec^2) and RSA (cm/sec^2) with 5% damping ratio for Sumatran subduction earthquakes

Period (s)	a_0	a_1	a_2	a_3	a_4	a_5	$\sigma_{\ln(Y)}$
PGV	2.369	2.0852	-0.23564	-0.87906	-0.001363	0.0001189	0.3478
PGA	3.882	1.8988	-0.11736	-1.00000	-0.001741	0.0000776	0.2379
0.50	4.068	1.9257	-0.12435	-0.99864	-0.001790	0.0000564	0.2410
0.60	4.439	1.9094	-0.13693	-0.99474	-0.002462	0.0001051	0.2496
0.70	4.836	1.8308	-0.13510	-0.99950	-0.003323	0.0001945	0.2565
0.80	4.978	1.8570	-0.12887	-1.00000	-0.003054	0.0001475	0.2626
0.90	5.108	1.9314	-0.13954	-0.98621	-0.002986	0.0001075	0.2424
1.00	4.973	1.9547	-0.13913	-0.97603	-0.002851	0.0001106	0.2343
1.20	2.729	2.0316	-0.13658	-0.60751	-0.002570	0.0000409	0.2436
1.50	2.421	1.8960	-0.07075	-0.59262	-0.002453	0.0000668	0.2614
2.00	2.670	1.8182	-0.07657	-0.62089	-0.002190	0.0000674	0.2780
3.00	1.716	1.7922	-0.01895	-0.61167	-0.001177	0.0000121	0.2944
5.00	-0.060	1.8694	-0.09103	-0.32688	-0.001765	0.0000529	0.3963
7.00	0.518	2.1948	-0.24519	-0.47529	-0.001064	0.0000189	0.4206
10.00	0.044	2.3081	-0.29060	-0.50356	-0.000848	0.0000125	0.5183
15.00	-0.525	2.5297	-0.41930	-0.52777	-0.001454	0.0001435	0.4495
20.00	-1.695	2.5197	-0.42807	-0.42096	-0.001575	0.0001498	0.4543
30.00	-2.805	2.6640	-0.42674	-0.43304	-0.001576	0.0001568	0.3686
50.00	-4.340	2.2968	-0.27844	-0.38291	-0.002564	0.0002540	0.3946

The resulting attenuation relationship for PGA is plotted in Figure 3, together with the simulated data. The figure shows that the derived attenuation relationship matches closely with the simulated data, indicating the adequacy of the functional form given in Equation (1).

Validation of the Attenuation Relationship Derived

The ground-motion attenuation relationships above were derived based solely on synthetic seismograms. It is therefore necessary to validate these attenuation models. The ground motions recorded in Singapore from the twelve significant earthquakes are used to validate the attenuation relationships. Geometric-mean of pseudo-acceleration response spectra (5% damping ratio) of these events are plotted in Figure 4 with think solid lines. The acceleration response spectra estimated using the derived attenuation relationship are shown by three lines denoted as "estimated" in each panel of Figure 4. The solid line in the middle indicates the mean spectrum, while the two enclosing dashed lines reflect the mean ± one standard deviation spectra. Note that the standard deviation values used are the ones that include both the uncertainty in source and path parameters, namely the values in Table 2 plus 0.2. The recorded spectra generally fall within the mean ± one standard deviation spectra for most of the events, indicating that the derived spectral attenuation relationship can predict actual recorded spectra within an acceptable level of uncertainty.

The spectra resulting from six existing attenuation relationships are to be plotted in Figure 4 to study if they can be extrapolated to predict spectra recorded in Singapore from Sumatran subduction earthquakes. Before comparing the spectra predicted by the six attenuation relationships with the recorded spectra, some adjustments have to be made with regards to difference in source-site distance definition and site effect.

In Figure 4, it can be seen that spectra calculated based on the attenuation relationships of Youngs *et al.* (1997), Gregor *et al*. (2002), Kanno *et al*. (2006) and Lin and Lee (2008) overestimate the recorded spectra in all the twelve events by one-order of magnitude. The resulting spectra from Gregor *et al*. (2002) for earthquakes with $M_w \leq 7$ have jagged shape, indicating that the attenuation relationship was derived only for large-magnitude subduction earthquakes and should not be extrapolated to lower magnitude range. Petersen *et al*. (2004) used a scaled-down attenuation relationship from Youngs *et al*. (1997) in a probabilistic seismic hazard analysis for Sumatra and peninsular Malaysia. The distance-dependent scaling factor of exp[0.0038(R-200)] was obtained by fitting the predicted spectral values at a natural period of 1 s from Youngs *et al.* (1997) to the actual data recorded in Singapore from Sumatran subduction earthquakes (Petersen *et al*. 2004). Therefore, the resulting spectra have identical shape with those from Youngs *et al.* (1997), and fit well with the recorded spectral values at the natural period of 1 s.

Among the six existing attenuation relationships, only the ones derived by Atkinson and Boore (2003) and Kanno *et al*. (2006) produces spectra with consistent shape to that of the recorded ones. It predicts spectra with a long predominant natural period of 2 s, which agrees well with that shown in the recorded spectra and consistent with the values expected for distant earthquakes (Megawati and Pan 2009). The other four attenuation relationships produce spectra with short predominant natural periods, below 0.6 s, which seem too short for distant earthquakes. It shows that these attenuation relationships were not well constrained at long distance and they are only meant for near-field earthquakes although the data used covered up to a distance of 500 km.

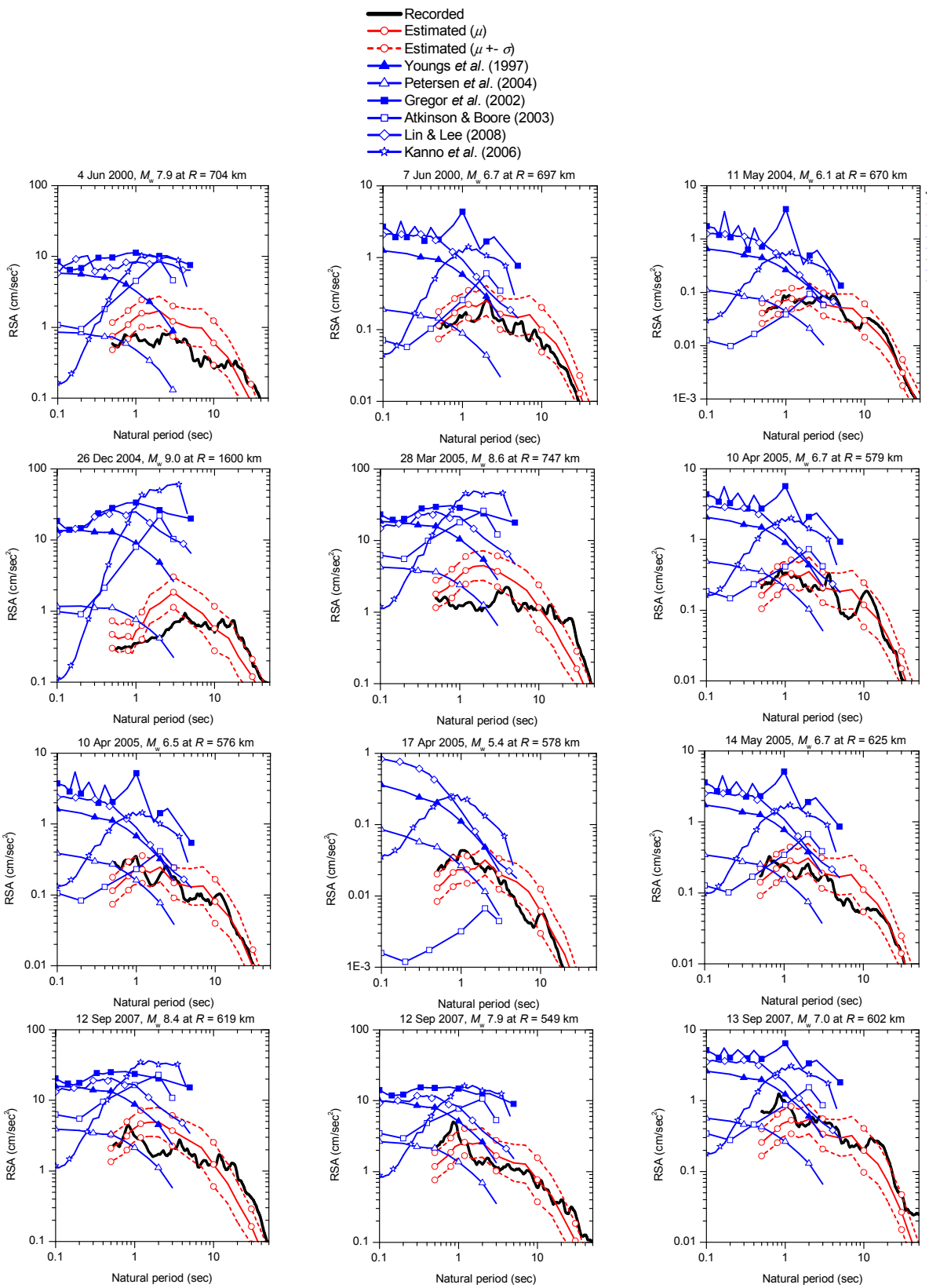

Figure 4. Recorded and estimated acceleration response spectra (5% damping ratio) of the twelve significant earthquakes.

References

Atkinson, G. M., D. M. Boore, 2003. Empirical ground-motion relations for subduction-zone earthquakes and their application to Cascadia and other regions. *Bulletin of the Seismological Society of America* 93, 1703-1729.

Boore, D. M., W. B. Joyner, 1997. Site amplifications for generic rock sites. *Bullettin of the Seismological Society of America* 87, 327-341.

Briggs, R. W., K. Sieh, A. J. Meltzner, D. Natawidjaja, J. Galetzka, B. Suwargadi, Y. J. Hsu, M. Simons, N. Hananto, I. Suprihanto, D. Prayudi, J. P. Avouac, L. Prawirodirdjo, Y. Bock, 2006. Deformation and slip along the Sunda Megathrust in the great 2005 Nias-Simeulue earthquake. *Science* 311, 1897-1901.

Chlieh, M., J. P. Avouac, V. Hjorleifsdottir, T. R. A. Song, C. Ji, K. Sieh, A. Sladen, H. Hebert, L. Prawirodirdjo, Y. Bock, J. Galetzka, 2007. Coseismic slip and afterslip of the great M_w 9.15 Sumatra-Andaman earthquake of 2004. *Bulletin of the Seismological Society of America* 97, S152-S173.

Fukushima, Y., 1996. Scaling relations for strong ground motion prediction models with M^2 terms. *Bulletin of the Seismological Society of America* 86, 329-336.

Gregor, N. J., W. J. Silva, I. G. Wong, R. R. Youngs, 2002. Ground-motion attenuation relationships for Cascadia subduction zone megathrust earthquakes based on a stochastic finite-fault model. *Bulletin of the Seismological Society of America* 92, 1923-1932.

Kanno, T., A. Narita, N. Morikawa, H. Fujiwara, Y. Fukushima, 2006. A new attenuation relation for strong ground motion in Japan based on recorded data. *Bulletin of the Seismological Society of America* 96, 879-897.

Lin, P. S., C. T. Lee, 2008. Ground-motion attenuation relationships for subduction-zone earthquakes in Northeastern Taiwan. *Bulletin of the Seismological Society of America* 98, 220-240.

Megawati, K., T. C. Pan, 2009. Regional seismic hazard posed by the Mentawai segment of the Sumatran megathrust. *Bulletin of the Seismological Society of America* 99, 566-584.

Natawidjaja, D. H., K. Sieh, M. Chlieh, J. Galetzka, B. W. Suwargadi, H. Cheng, R. L. Edwards, J. P. Avouac, S. N. Ward, 2006. Source parameters of the great Sumatran megathrust earthquakes of 1797 and 1833 inferred from coral microatolls. *Journal of Geophysical Research* 111, Art. No. B06403.

Pan, T. C., and J. C. Sun, 1996. Historical earthquakes felt in Singapore, *Bulletin of the Seismological Society of America* 86, 1173-1178.

Petersen, M. D., J. Dewey, S. Hartzell, C. Mueller, S. Harmsen, A. D. Frankel, K. Rukstales, 2004. Probabilistic seismic hazard analysis for Sumatra, Indonesia and across the southern Malaysian peninsula. *Tectonophysics* 390, 141-158.

Wells, D. L., K. J. Coppersmith, 1994. New empirical relationships among magnitude, rupture length, rupture width, rupture area, and surface displacement. *Bulletin of the Seismological Society of America* 84, 974-1002.

Youngs, R. R., S. J. Chiou, W. J. Silva, J. R. Humphrey, 1997. Strong ground motion attenuation relationships for subduction zone earthquakes. *Seismological Research Letters* 68, 58-73.